RAD21L, a novel cohesin subunit implicated in linking homologous chromosomes in mammalian meiosis

Jibak Lee and Tatsuya Hirano

Chromosome Dynamics Laboratory, RIKEN Advanced Science Institute, 2-1 Hirosawa, Wako, Saitama 351-0198, Japan

Cohesins are multi-subunit protein complexes that regulate sister chromatid cohesion during mitosis and meiosis. Here we identified a novel kleisin subunit of cohesins, RAD21L, which is conserved among vertebrates. In mice, RAD21L is expressed exclusively in early meiosis: it apparently replaces RAD21 in premeiotic S phase, becomes detectable on the axial elements in leptotene, and stays on the axial/lateral elements until mid pachytene. RAD21L then disappears, and is replaced with RAD21. This behavior of RAD21L is unique and distinct from that of REC8, another meiosis-specific kleisin subunit. Remarkably, the disappearance of RAD21L at mid pachytene correlates with the completion of DNA double-strand break repair and the formation of crossovers as judged by colabeling with molecular markers, γ-H2AX, MSH4, and MLH1. RAD21L associates with SMC3, STAG3, and either SMC1α or SMC1β. Our results suggest that cohesin complexes containing RAD21L may be involved in synapsis initiation and crossover recombination between homologous chromosomes.

Introduction

Meiosis is a sexual reproduction process in which chromosome number is halved from the diploid in a parental cell to the haploid in daughter cells. To this end, two successive meiotic divisions occur after a single round of DNA replication. Meiotic chromosomes exhibit highly unique behaviors particularly in the first meiotic division (meiosis I). Homologous chromosomes pair, synapse, and recombine with their partners during prophase I. The chiasmata resulting from crossover recombination, in conjunction with arm cohesion between sister chromatids, make physical connections between homologous chromosomes, leading to the formation of bivalent chromosomes by metaphase I. At the onset of anaphase I, resolution of the inter-sister arm cohesion causes separation of homologous chromosomes while sister chromatids are kept attached at their centromere regions. The sister chromatids eventually separate from each other when the centromeric cohesion is resolved in meiosis II (Miyazaki and Orr-Weaver, 1994; Petronczki et al., 2003). To achieve this highly intricate series of chromosomal events, meiotically dividing cells are equipped with specialized components and regulatory mechanisms.

Meiotic recombination is initiated by DNA double-strand breaks (DSBs) created by the topoisomerase II–like protein SPO11 (Keeney, 2001). The DSBs are then processed in a series of recombination events, and eventually converted into two products, crossovers and noncrossovers (Page and Hawley, 2004; de Boer and Heyting, 2006). At first, the DSBs are resected to yield 3′ single-strand DNA ends, which in turn allow single-end invasion mediated by RAD51 and DMC1 (Schwacha and Kleckner, 1997; Hunter and Kleckner, 2001; Keeney, 2001). In mammalian meiosis, the early recombination intermediates containing RAD51 and DMC1 are gradually replaced first by middle intermediates containing MSH4 (a homologue of *Escherichia coli* MutS) and eventually by late intermediates containing MLH1 (a MutL homologue; Plug et al., 1998; Santucci-Darmanin et al., 2000). MLH1 is essential for crossover recombination, appearing only at the crossover sites but not at the noncrossover sites during pachytene (Anderson et al., 1999; Santucci-Darmanin et al., 2000; Guillon et al., 2005).

In many organisms, the pairing, synapsis, and recombination of homologous chromosomes occurs in parallel with the

Correspondence to Tatsuya Hirano: hiranot@riken.jp

Abbreviations used in this paper: AE, axial element; CE, central element; DSB, DNA double-strand break; γ-H2AX, histone H2AX phosphorylated at Ser139; LE, lateral element; SC, synaptonemal complex.

The Rockefeller University Press $30.00
J. Cell Biol. Vol. 192 No. 2 263–276
www.jcb.org/cgi/doi/10.1083/jcb.201008005

formation of some cytologically discernible structures (Page and Hawley, 2004). The so-called axial elements (AEs) assemble along each chromosome in the leptotene stage, and start to pair and synapse in zygotene, thereby initiating the assembly of the synaptonemal complex (SC). In pachytene, synapsis completes along their entire length of the lateral elements (LEs; an alternative name for the AE after synapsis). The resulting SC has a tripartite structure with two LEs connected by transverse filaments called the central element (CE), which then starts to disassemble in diplotene. In mammals, SYCP2 and SYCP3 are the main components of the AE/LE whereas SYCP1 constitutes the CE (Meuwissen et al., 1992; Dobson et al., 1994; Offenberg et al., 1998), and all these components are essential for proper progression of meiosis. Both *SYCP2*- and *SYCP3*-deficient male mice fail to form the AEs and are sterile due to massive apoptotic cell death at or before pachytene (Yuan et al., 2000; Yang et al., 2006). In *SYCP1*-deficient mice the AEs are formed and aligned normally, but neither synapse nor form MLH1 foci (de Vries et al., 2005).

A series of recent studies has demonstrated that multisubunit protein complexes, known as cohesins, play key roles in many aspects of meiotic chromosome dynamics. The canonical cohesin complex, originally identified as a central player in sister chromatid cohesion in mitosis, is composed of four subunits: two structural maintenance of chromosomes (SMC) subunits (SMC1α and SMC3) and two non-SMC subunits (RAD21 [known as Scc1/Mcd1 in budding yeast] and SA/STAG [known as Scc3 in the yeast]; Hirano, 2006; Nasmyth and Haering, 2009). In mammals, mitotic cells possess two types of cohesin complexes with different SA subunits (i.e., SMC1α–SMC3–RAD21–SA1 and SMC1α–SMC3–RAD21–SA2; Losada et al., 2000). On the other hand, meiotic cells, such as spermatocytes and oocytes, express at least three additional subunits, SMC1β (an SMC1α paralog), REC8 (a RAD21 paralog), and STAG3 (an SA1/SA2 paralog). Many if not all of these cohesin subunits have been localized along the AE/LEs of the SC (Eijpe et al., 2000, 2003; Prieto et al., 2001, 2002, 2004; Revenkova et al., 2001; Lee et al., 2003; Xu et al., 2004). Among them, REC8 and SMC1β have been shown to be essential for proper assembly of the SC and crossover recombination (Revenkova et al., 2004; Xu et al., 2005). Expression of these meiosis-specific subunits would predict the occurrence of a wide variety of different cohesin complexes with different subunit compositions in meiotic cells. However, the biochemical nature of these putative complexes is not fully understood.

Most eukaryotic species possess two kleisin subunits, RAD21 and REC8. Here we report, for the first time, the presence of the third kleisin subunit, designated RAD21L, in mammals. The orthologues of RAD21L are found in vertebrates, but not in invertebrate species. RAD21L is specifically expressed in meiotic cells (spermatocytes and oocytes), and localizes along the AE/LEs of the SC from leptotene to mid pachytene. One of the most striking features of RAD21L is that, unlike any other cohesin subunit, it dissociates from the SC at mid pachytene and is not detectable in the subsequent stages of meiosis. We provide several lines of evidence suggesting that RAD21L may be involved in synapsis initiation and crossover recombination between homologous chromosomes. The current results allow us to propose a model in which the spatiotemporal regulation of a variety of cohesin complexes contributes to progression of the elaborate sequence of chromosomal events during meiotic prophase I.

Results

Identification of the gene encoding a novel kleisin subunit of cohesins in vertebrates

In the course of BLAST searches using the mouse RAD21 sequence as a query, we noticed that vertebrate genomes encode a protein closely related, but not identical, to RAD21 of each species. In the current study, we refer to this novel gene product as RAD21L (RAD21-like protein). A single copy of the *RAD21L* gene was found in each of the vertebrate genomes sequenced so far. *RAD21L* was, however, not found in any of the invertebrate species including amphioxus, living proxies for the chordate ancestor (Putnam et al., 2008). A phylogenetic analysis of kleisin subunits of cohesins among vertebrates indicated that they were categorized into three subfamilies, namely, RAD21, RAD21L, and REC8, and that RAD21L was much closer to RAD21 than to REC8 (Fig. 1 A). An alignment of the amino acid sequences of mouse RAD21, RAD21L, and REC8 is shown in Fig. S1. RAD21L displayed 44% and 17% identity to RAD21 and REC8, respectively, in total length: conserved residues were clustered into two winged-helix domains located at their N and C termini (Fig. 1 B). All the information taken together, it is reasonable to speculate that the *RAD21L* gene has diverged from the *RAD21* gene immediately after the appearance of vertebrates. It should be noted that, unlike RAD21L, REC8 is found in most eukaryotic organisms.

RAD21L is expressed in a limited population of meiotic cells

We cloned a cDNA for RAD21L from a mouse testis cDNA library by PCR (see Materials and methods). In a Northern blot analysis using mRNAs isolated from various mouse organs, virtually no signal for *RAD21L* was detectable (unpublished data). Under the same condition, *RAD21* mRNA was detectable ubiquitously and *REC8* mRNA was found only in testes, as described previously (Lee et al., 2002). To detect a supposedly low level of *RAD21L* mRNA, we then performed quantitative PCR (qPCR) using cDNAs prepared from liver, spleen, and testis (Fig. 2 A). Consistent with the results of the Northern analysis, *RAD21* mRNA (along with *GAPDH* mRNA used as a positive control) was readily detectable in all three organs whereas *REC8* mRNA was detected only in testis, but hardly in liver or spleen. Most importantly, this approach allowed us to detect *RAD21L* mRNA in testis, but not in the others. The cycle numbers and the efficiencies of amplification in the real-time PCR allowed us to roughly estimate the relative abundance of mRNAs for each gene (see Materials and methods). The level of *RAD21L* mRNA was estimated to be extremely low even in testis, being <1% of that of *RAD21* mRNA. In contrast, the level of *REC8* mRNA was roughly equivalent (>60%) to that of *RAD21* mRNA in testis. These results reveal that the expression of *RAD21L* is testis specific, and may be limited in specific cell types present in the testis organ.

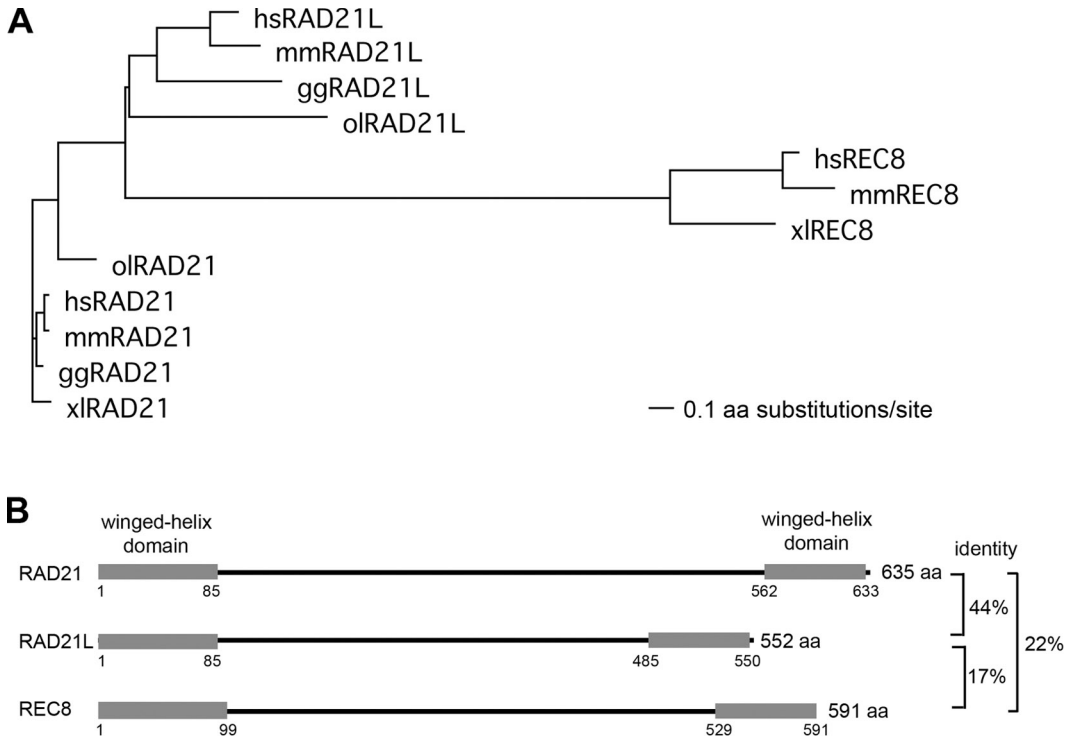

Figure 1. **RAD21L is the third kleisin subunit of cohesins conserved among vertebrate species.** (A) A phylogenetic tree of kleisin subunits of cohesins among vertebrates was constructed by using ClustalW and TreeView programs. The GenBank/EMBL/DDBJ accession nos. or Ensemble database nos. are as follows; hsRAD21 (BC050381), mmRAD21 (AK163992), ggRAD21 (AJ719731), xlRAD21 (BC077991), olRAD21 (AB115697), hsRAD21L (BC157891), mmRAD21L (AB574185), ggRAD21L (ENSGALG00000006186), olRAD21L (ENSORLT00000018324), hsREC8 (BC010887), mmREC8 (BC052155), and xlREC8 (BC087346). The nomenclatures of species are as follows; hs, *Homo sapiens*; mm, *Mus musculus*; gg, *Gallus gallus* (chicken); xl, *Xenopus laevis*; ol, *Oryzias latipes* (medaka fish). (B) Schematic representation of the primary structures of three different kleisin subunits of cohesins in the mouse. Gray boxes indicate winged-helix domains conserved among the kleisin family of proteins.

To analyze RAD21L at the protein level, rabbit and rat polyclonal antibodies were raised against its C-terminal recombinant fragment. Both antibodies recognized a polypeptide with an apparent mol wt of ~95 kD on an immunoblot against a testis extract (Fig. 2 B). The size was substantially bigger than the predicted one (~63 kD), a characteristic commonly observed among many kleisin subunits. We then performed an immunoblot analysis against extracts prepared from various mouse organs using a set of antibodies against the kleisin subunits and SMC3 (a core subunit of cohesins; Fig. 2 C). Although RAD21 and SMC3 were detected in all the organs examined, RAD21L and REC8 were found only in testis. RAD21L was also found in ovary as judged by immunoblot analysis after immunoprecipitation using an anti-RAD21L antibody (unpublished data). We therefore conclude that RAD21L is specifically expressed in both male and female gonads.

To determine which cell types in the gonads might be positive for RAD21L, frozen sections of the ovary and testis were immunofluorescently labeled with anti-RAD21L (Fig. 2 D). To identify meiotic cells in the gonads, an antibody against SYCP3 (a component of the AE/LE) was used simultaneously. We found that, in both gonads, RAD21L was detectable only in the cell population positive for SYCP3. Virtually no specific signal of RAD21L was found in somatic cells, spermatogonia (premeiotic cells), or spermatids (post-meiotic cells). Thus, RAD21L is specifically expressed in meiotic cells in both male and female. The big difference in the mRNA level between *RAD21L* and the other kleisin genes, as judged by the quantitative PCR, might be attributed not only to the exclusive expression of *RAD21L* in meiotic cells but also to the high abundance of *RAD21* and *REC8* mRNAs in spermatids (Lee et al., 2002).

RAD21 and RAD21L are expressed in a mutually exclusive manner during meiosis

To directly compare the expression timing and distribution of RAD21 and RAD21L during meiosis, we performed immunofluorescent labeling of testis sections with specific antibodies to RAD21 and RAD21L (Fig. 3 A). In the testis, spermatogenesis proceeds in a centripetal direction from the inner basement membrane (Fig. 3 A, a and e; green dashed lines) to the lumen of the seminiferous tubules. RAD21L was specifically detected only in some population of spermatocytes near the basement membrane (Fig. 3 A, f and h; white arrowheads). In contrast, the signal of RAD21 was prominent in somatic cells outside the seminiferous tubules or in spermatogonia, and was also detected in some spermatocytes localizing away from the basement membrane (Fig. 3 A, g and h; yellow arrowheads). Remarkably, however, the RAD21 signal was hardly detectable in the RAD21L-positive spermatocytes. We also performed immunofluorescent colabeling of RAD21 and RAD21L on nuclear spreads of testicular cells (Fig. 3 B). Again, most of the RAD21L-positive spermatocyte nuclei were not labeled with RAD21, and vice versa (Fig. 3 B, a–d). In a small population of pachytene-like nuclei, however, faint signals for both

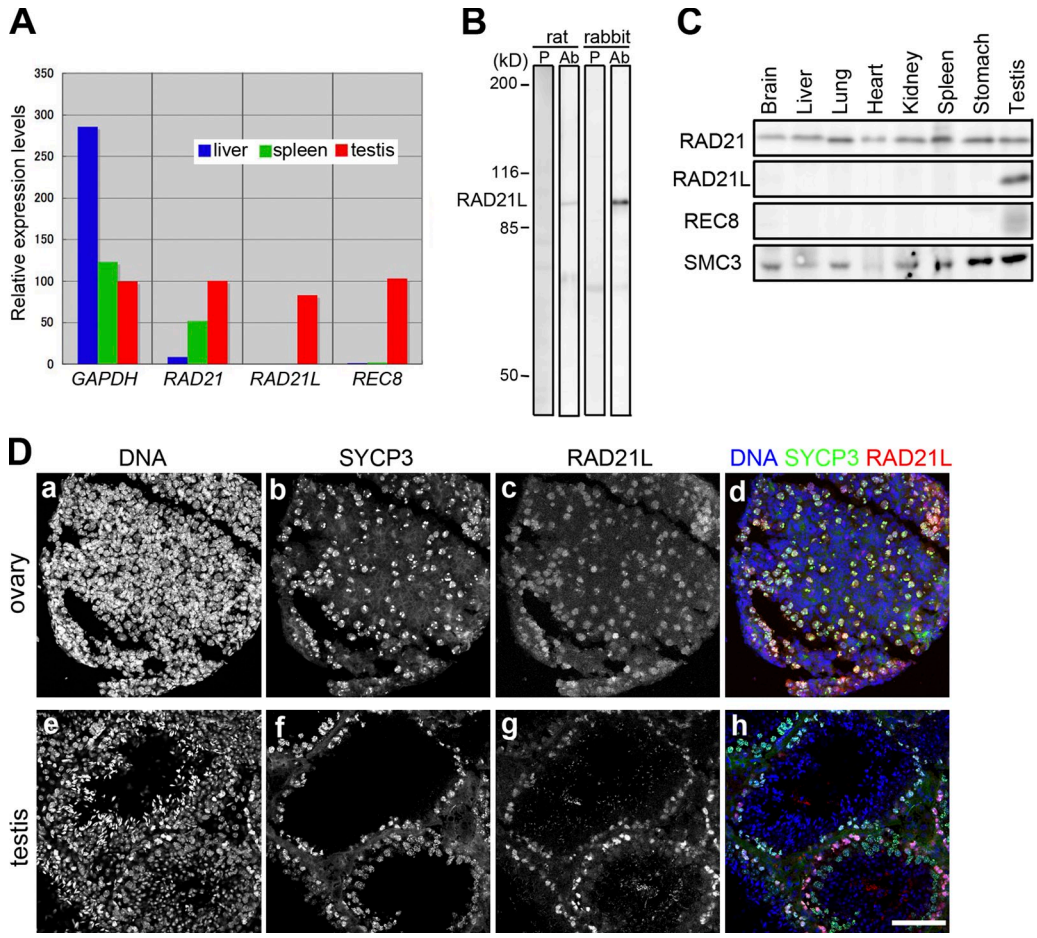

Figure 2. **Specific expression of RAD21L in both male and female gonads.** (A) Relative transcript levels of *RAD21*, *RAD21L*, *REC8*, and *GAPDH* (an internal control) in mouse liver, spleen, and testis were assessed by real-time RT-PCR. For each gene, 100-fold diluted, 10-fold diluted, or undiluted cDNAs from testis were used for making a standard curve, and all values are shown in comparison with values obtained in the control samples using the undiluted cDNAs from testis. (B) Immunoblot analysis of a testis extract using rat and rabbit antibodies (Ab) raised against RAD21L or preimmune sera (P). (C) Immunoblot analysis of extracts from various mouse organs with rabbit polyclonal antibodies against the different kleisin subunits and SMC3. (D) Immunofluorescent labeling of frozen sections of fetal ovary (18.5 d post-coitum) (a–d) and adult testis (e–h) with mouse polyclonal anti-SYCP3 (b and f) and rat polyclonal anti-RAD21L (c and g) antibodies. DNA was counterstained with Hoechst 34580 (a and e) and merged images are shown (d and h). Bar, 100 µm.

RAD21 and RAD21L were detectable (Fig. 3 B, e–h). Interestingly, the two signals hardly overlapped with each other and apparently alternated along the SC (Fig. 3 B, f′–h′), most likely corresponding to the transition stage from RAD21L to RAD21.

These results revealed that RAD21L largely replaces RAD21 during early stages of prophase I, and that, conversely, RAD21 reappears in later stages of prophase I to replace RAD21L. Two previous studies had reported conflicting results regarding the temporal expression of RAD21 in mouse spermatocytes: one study reported a transient appearance of RAD21 at a late stage of prophase I (Prieto et al., 2002), whereas the other reported its persistent presence throughout prophase I (Xu et al., 2004). The former study was more consistent with our observation reported here.

RAD21L appears from premeiotic S phase and disappears at mid pachytene

To examine when RAD21L starts to appear in meiotic cells, nuclear spreads of testicular cells were immunofluorescently colabeled with antibodies against RAD21L and PCNA, a marker for S phase (Bravo and Macdonald-Bravo, 1987). We found that the nuclei of some spermatocytes were simultaneously positive for RAD21L and PCNA (Fig. S2), suggesting that RAD21L is expressed from premeiotic S phase, as had been observed for REC8 (Eijpe et al., 2003).

To determine the exact stages in which RAD21L appears in meiotic chromosomes, nuclear spreads of spermatocytes were colabeled with antibodies against RAD21L and SYCP3. In the leptotene stage when the AEs started forming, RAD21L was already present and localized along the AEs (Fig. 4, a–d). In the zygotene stage when synapsis initiated, RAD21L was detected as dot- or thread-like signals along the AE/LEs of the SC being assembled (Fig. 4, e–h). Notably, the signals of RAD21L appeared enriched on synaptic sites where two AEs made a contact to initiate synapsis (Fig. 4, h′ and h′′; arrowheads). In pachytene when the synapsis was apparently completed, the RAD21L signals distributed evenly along the entire length of the SC in some nuclei (Fig. 4, i–l), and were hardly detectable in others (Fig. 4, m–p). The RAD21L signals were undetectable in later meiotic stages, from diplotene (Fig. 4, q–t) through metaphase I (not depicted). Taken together with the results from testis sections (Fig. 3), these

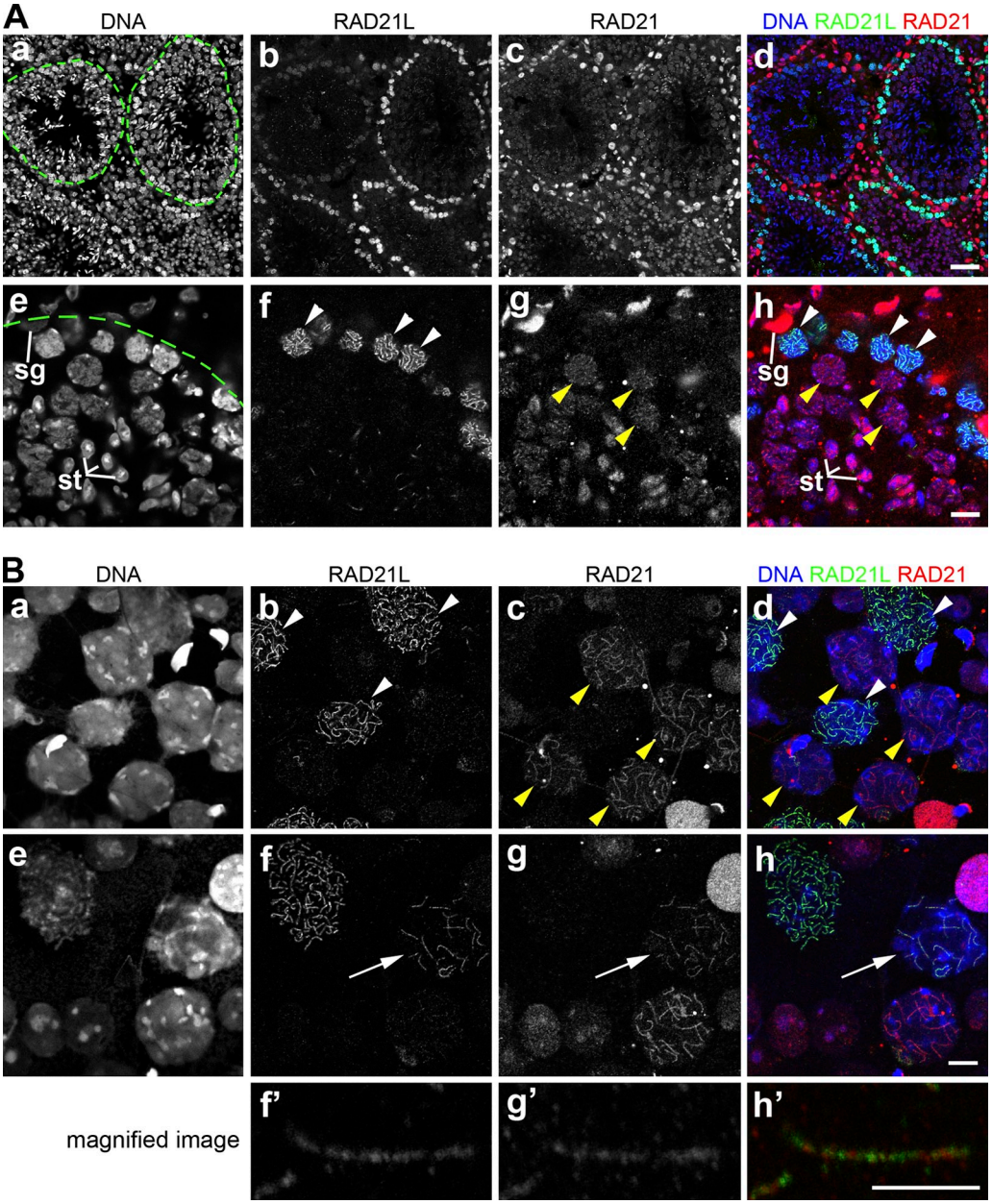

Figure 3. **RAD21 and RAD21L are detected in a mutually exclusive manner in mouse testicular cells.** (A) Frozen sections of adult testis were immunofluorescently labeled with rat polyclonal anti-RAD21L (b and f) and rabbit polyclonal anti-RAD21 (c and d) antibodies. Note that spermatocytes located near the fibrous capsule (a and e; green dashed lines) of seminiferous tubules were RAD21L-positive cells (f and h; white arrowheads), whereas spermatocytes located relatively close to the center of the tubules are RAD21-positive cells (g and h; yellow arrowheads). In e and h, sg and st indicate spermatogonium and spermatid, respectively. DNA was counterstained with Hoechst 34580 (a and e) and merged images are shown (d and h). An overview image (a–d) and a magnified image (e–h) of different testis sections are shown. Bars: (d) 50 µm; (h) 10 µm. (B) Nuclear spreads from testicular cells were immunofluorescently labeled with rat polyclonal anti-RAD21L (b and f) and rabbit polyclonal anti-RAD21 (c and g) antibodies. Note that spermatocyte nuclei were exclusively labeled with either anti-RAD21L (b and d; white arrowheads) or anti-RAD21 (c and d; yellow arrowheads) antibody, whereas a nucleus (f–h; white arrow) was faintly labeled with both antibodies. DNA was counterstained with Hoechst 34580 (a and e) and merged images are shown (d and h). Also shown are magnified images of a chromosome colabeled with the two antibodies (f'–h'). Bars: (h) 10 µm; (h') 5 µm.

data strongly suggested that RAD21L disappears from the SC in the middle of the pachytene stage (i.e., mid pachytene). In fact, this conclusion was supported by a colabeling experiment with antibodies against MSH4 and MLH1 (see below, Fig. S3 B, and Fig. 6 B), whose signals had been used to assess sub-stages within pachytene (Plug et al., 1998; Santucci-Darmanin et al., 2000). It was somewhat surprising for us to find that RAD21L disappeared from the meiotic chromosomes at mid pachytene when the SC was still intact as judged by SYCP3 labeling. This behavior in early prophase I is absolutely unique to RAD21L, being in striking contrast to the behaviors of known cohesin subunits.

Differential distribution of RAD21L and REC8 on the synaptonemal complex

Previous studies had shown that REC8 is localized along AE/LEs of the SC from leptotene to diplotene (Eijpe et al., 2003;

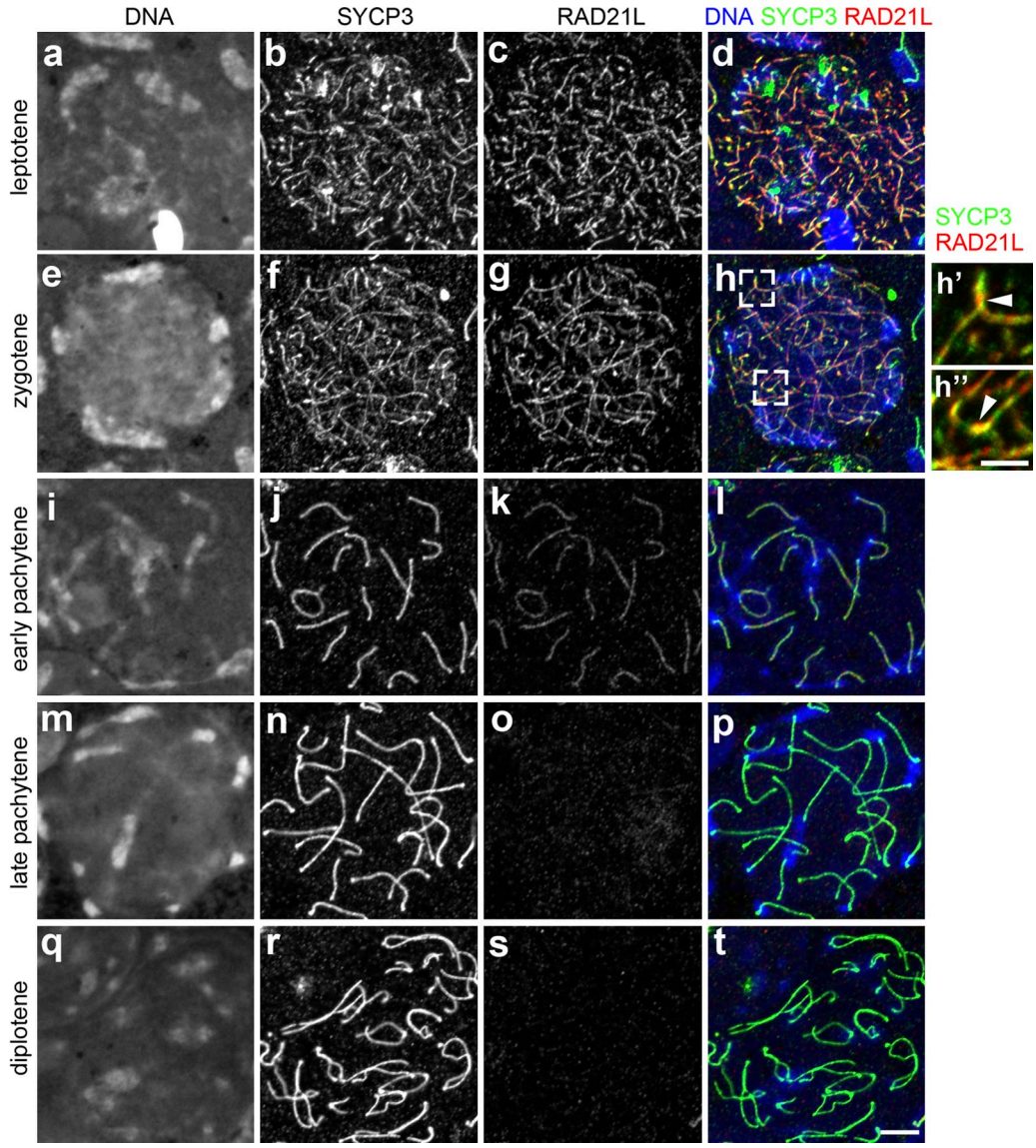

Figure 4. **The appearance of RAD21L on meiotic chromosomes is strictly confined in early stages of meiotic prophase I.** Nuclear spreads from testicular cells were prepared and immunofluorescently labeled with rat polyclonal anti-RAD21L (c, g, k, o, and s) and mouse polyclonal anti-SYCP3 (b, f, j, n, and r) antibodies. DNA was counterstained with Hoechst 34580 (a, e, i, m, and q) and merged images are shown (d, h, l, p, and t). Some of the bivalents in h are enlarged in h′ and h′′. Bars: (x) 5 µm; (h′′) 2 µm.

Lee et al., 2003). To directly compare the distribution of RAD21L with that of REC8, nuclear spreads of spermatocytes were co-labeled with antibodies against the two meiotic kleisins. Both RAD21L and REC8 signals first became detectable as arrays of dot-like structures in leptotene (Fig. 5, a–d), and were gradually lined up into more continuous structures from zygotene (Fig. 5, e–h) through early pachytene (Fig. 5, i–l). In diplotene, the RAD21L signal was no longer detectable whereas REC8 was retained on the desynapsed LEs (Fig. 5, m–p). Very importantly, although RAD21L and REC8 largely coexisted along the AE/LEs from leptotene to early pachytene, their detailed localizations were distinct from each other. Indeed, magnified images revealed that the signals of RAD21L and REC8 did not overlap and apparently alternate along the AE/LEs at zygotene (Fig. 5, f′–h′) and early pachytene (Fig. 5, j′–l′). These results provide the first line of evidence for the existence of alternating sub-chromosomal domains containing distinct kleisin subunits along meiotic chromosomes.

RAD21L disappears at mid pachytene coincidentally with crossover formation

To test whether the disappearance of RAD21L from meiotic chromosomes at mid pachytene might correlate with other chromosomal events, we performed colabeling experiments. We initially focused on the dynamics of histone H2AX phosphorylated at S139 (γ-H2AX). In addition to two strong signals of γ-H2AX that had been reported before, a hitherto unrecognized signal on the SC was noticed as described below. A strong and chromosome-wide signal of γ-H2AX first appeared in leptotene and zygotene (Fig. 6 A, a–d and e–h). This signal, which is thought to be dependent mostly on ATM in response to DSBs created by SPO11 (Mahadevaiah et al., 2001; Barchi et al., 2005;

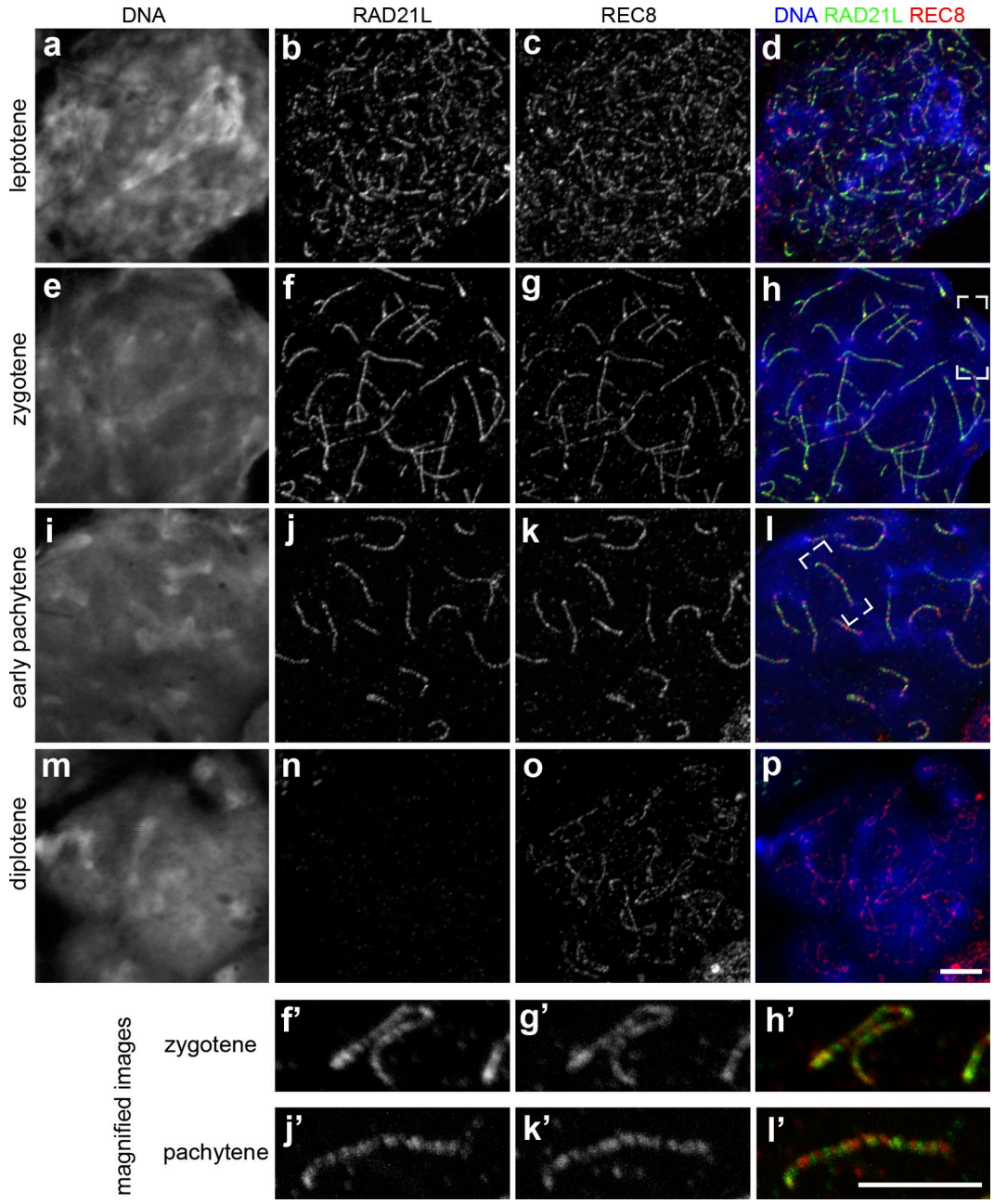

Figure 5. **Differential distributions of RAD21L and REC8 on the synaptonemal complex during meiotic prophase I.** Nuclear spreads from testicular cells were prepared and immunofluorescently labeled with rat polyclonal anti-RAD21L (b, f, j, n, f′, and j′) and rabbit polyclonal anti-REC8 (c, g, k, o, g′, and k′) antibodies. The regions indicated in h and l are magnified in f′–h′ and j′–k′, respectively. DNA was counterstained with Hoechst 34580 (a, e, i, and m) and merged images are shown (d, h, l, p, h′, and l′). Bar, 5 µm.

Bellani et al., 2005), largely disappeared in early pachytene, yet a sub-fraction was left along the proximity of the SC (Fig. 6, i–l). At the same time, the second population of strong γ-H2AX signals started to accumulate onto the XY sex chromosomes in early pachytene, as had been reported previously (Chicheportiche et al., 2007; Blanco-Rodríguez, 2009). This is an indicator of the formation of XY body, and is thought to be dependent on ATR (Turner et al., 2004). It was noteworthy that, although the γ-H2AX signal on XY body stayed robust throughout pachytene, the signal on the SC was weakened gradually around mid pachytene and lost almost completely by late pachytene (Fig. 6, m–p and q–t). The disappearance of γ-H2AX from the SC occurred highly coincidentally with that of RAD21L, raising the possibility that RAD21L might contribute, directly or indirectly, to processing of DSBs and/or completion of their repair.

To test this idea further, we next examined the temporal relationship between RAD21L signals and RAD51 foci, a marker for early recombination intermediates, or MSH4 foci, a marker for middle recombination intermediates. We found that RAD51 foci appeared in leptotene and largely disappeared in early pachytene, as had been reported previously (Plug et al., 1998; Tarsounas et al., 1999). The disappearance of RAD51 foci from

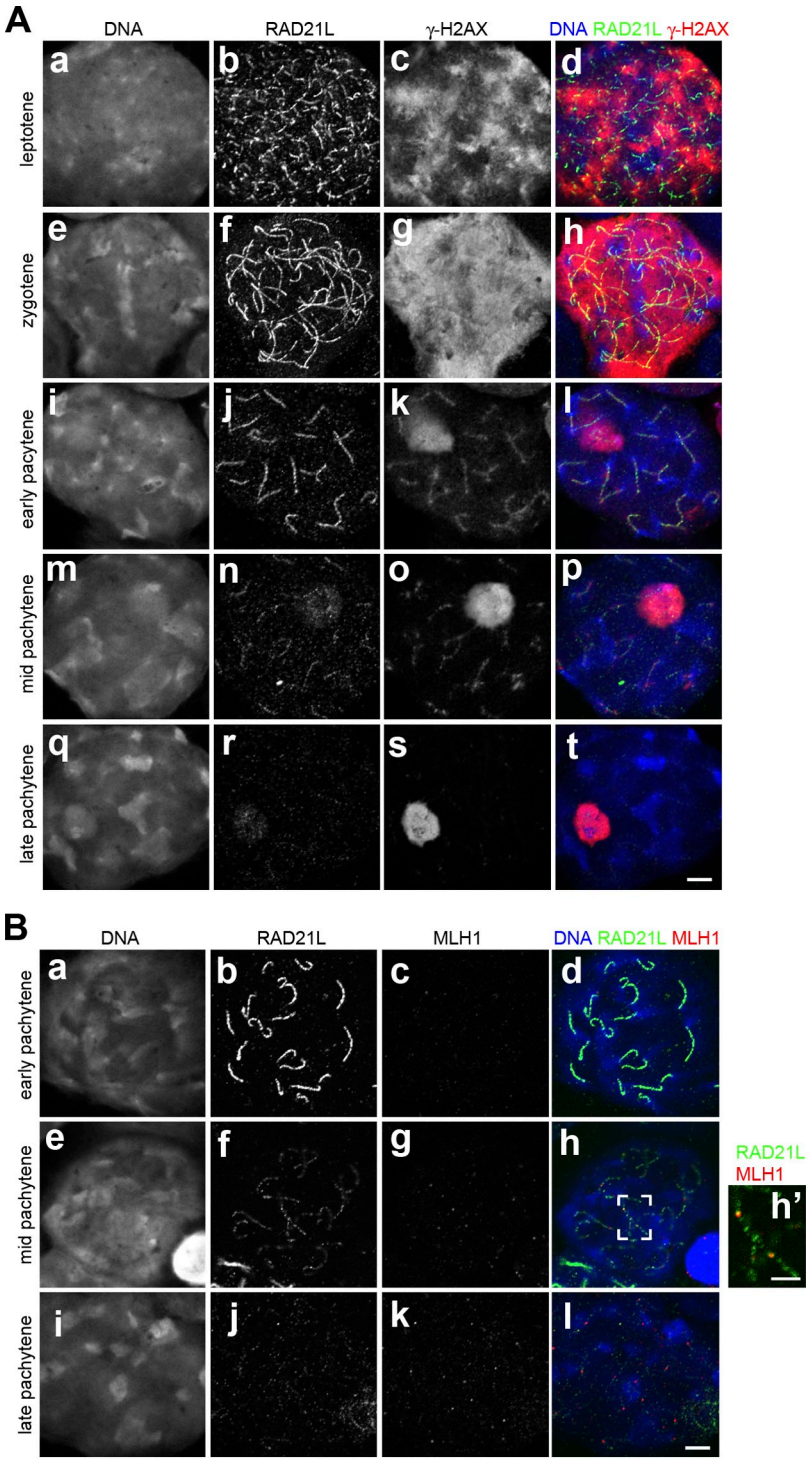

Figure 6. **Temporal correlation between the disappearance of RAD21L and other pachytene events.** (A) Nuclear spreads from testicular cells were prepared and subjected to immunofluorescent labeling with rat polyclonal anti-RAD21L (b, f, j, n, and r) and rabbit polyclonal anti–γ-H2AX (c, g, k, o, and s) antibodies. DNA was counterstained with Hoechst 34580 (a, e, i, m, and q) and merged images are shown (d, h, l, p, and t). Bar, 5 µm. (B) Nuclear spreads from testicular cells were immunofluorescently labeled with rat polyclonal anti-RAD21L (b, f, and j) and mouse monoclonal anti-MLH1 (c, g, and k) antibodies. DNA was counterstained with Hoechst 34580 (a, e, and i) and merged images are shown (d, h, and l). The region indicated in h is magnified in h′. Bars: (l) 5 µm; (h′) 2 µm.

meiotic chromosomes precedes the disappearance of RAD21L signals (Fig. S3 A). On the other hand, MSH4 foci were detected at late zygotene (unpublished data) and early pachytene on the SC, but not at late pachytene (Fig. S3 B), as had been reported previously (Santucci-Darmanin et al., 2000). The disappearance of RAD21L signals nicely correlated with that of MSH4 foci.

Finally, we looked at MLH1 foci, a marker for crossovers (Anderson et al., 1999). In early pachytene when RAD21L signals localized along the SC, MLH1 foci were rarely observed (Fig. 6 B, a–d). A few MLH foci started to appear in mid pachytene when the RAD21L signals got gradually reduced (Fig. 6 B, e–h and h′). The number of MLH1 foci increased in late pachytene when RAD21L was no longer detectable (Fig. 6 B, i–l). Thus, the disappearance of RAD21L from pachytene chromosomes correlates with the formation of crossovers.

Biochemical characterization of meiotic cohesin complexes in mice

Despite an extensive series of cytological studies, there have been only a few biochemical studies concerning multiple cohesin

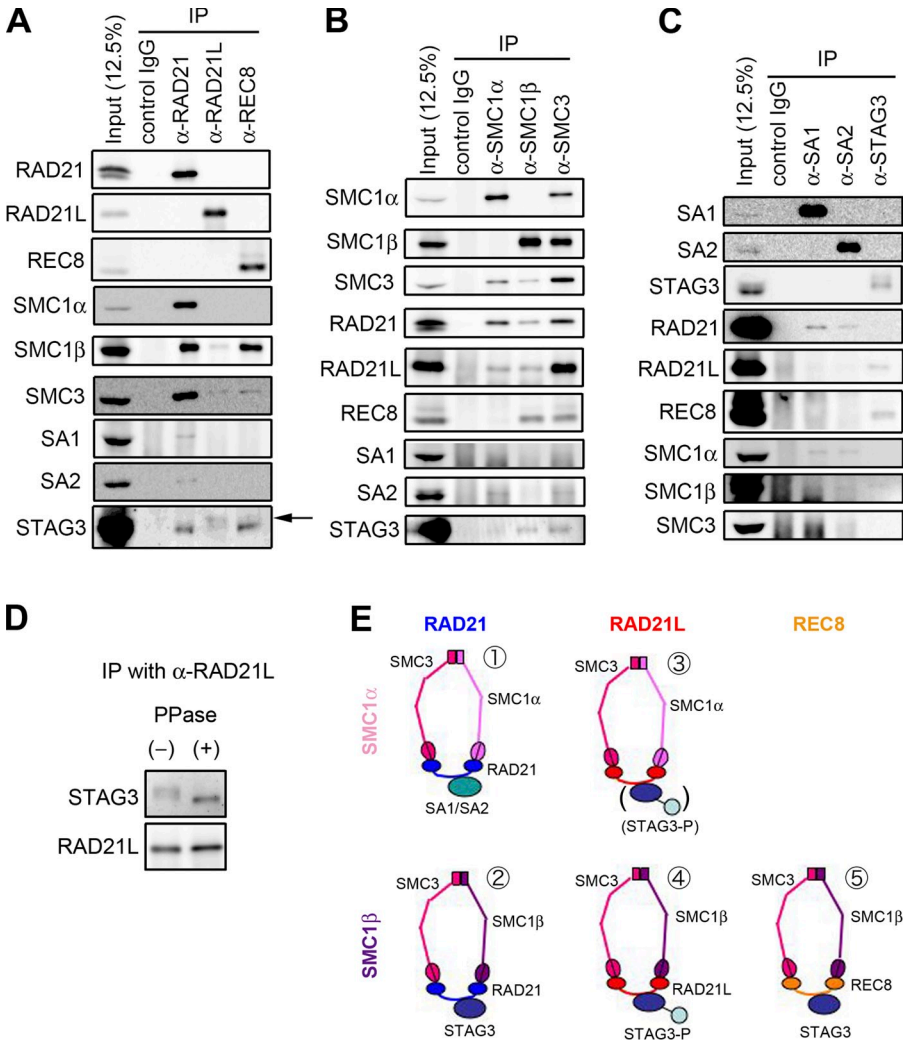

Figure 7. **Comprehensive immunoprecipitation analysis with antibodies against different cohesin subunits.** (A–C) Testis extracts were subjected to immunoprecipitations using antibodies against kleisin subunits (A), SMC subunits (B), and SA–STAG subunits (C). The precipitates, along with aliquots of the input fractions, were analyzed by immunoblotting with the antibodies indicated. The arrow in A indicates the phosphorylated form of STAG3 coprecipitated with RAD21L. (D) Immunoprecipitates obtained with anti-RAD21L antibody were treated with (+) or without (−) λ-PPase, and were analyzed by immunoblotting with antibodies indicated. (E) Putative subunit compositions of the cohesin complexes as revealed by our immunoprecipitation assays. The number assigned for each complex is also used in Fig. 8. STAG3 might not be included in the third cohesin complex (therefore shown in parentheses) because the association between SMC1α and STAG3 was hardly detectable in our assays.

complexes in mammalian meiosis (Lee et al., 2003; Revenkova et al., 2004; Suja and Barbero, 2009). As a consequence, we currently have very limited information about how many different combinations of subunits might create how many different types of cohesin complexes in meiotic cells. Our current discovery of RAD21L, a novel, putative subunit of cohesins, provides an additional layer of complexity to this problem. To clarify this important problem, we performed systematic coimmunoprecipitation assays with the antibodies to RAD21L as well as all known cohesin subunits, using an extract from testes.

In the first set of experiments, a testis extract was subjected to immunoprecipitation with antibodies against the three kleisin subunits, and the precipitates were analyzed by immunoblotting (Fig. 7 A). Only a single kleisin subunit was detected in each of the immunoprecipitates, indicating that different kleisin subunits do not coexist in any cohesin complexes. SMC1α was coprecipitated with RAD21 but with neither RAD21L nor REC8, whereas SMC1β (and SMC3) was coprecipitated with all three kleisins. The amounts of the SMC subunits coprecipitated with RAD21L were small in all cases, most likely reflecting the very limited amount of RAD21L present in the testis extract (Fig. 2; also see Fig. S4 A). SA1 and SA2 were coprecipitated only with RAD21, whereas STAG3, the STAG/SA subunit whose expression is limited to meiosis, was coprecipitated with all three kleisins. Interestingly, only the fraction of STAG3-coprecipitated RAD21L displayed a mobility shift (Fig. 7 A, arrow), which turned out to be dependent on phosphorylation (Fig. 7 D). In the next set of experiments, antibodies against three different SMC subunits were used for immunoprecipitation (Fig. 7 B). Anti-SMC3 antibody precipitated all subunits tested here (except SA1), and SMC1α and SMC1β were never coprecipitated with each other, indicating that either SMC1α–SMC3 or SMC1β–SMC3 represents the core subunit of all cohesin complexes. RAD21 and RAD21L associated with either SMC1α or SMC1β, whereas REC8 associated with SMC1β only. Thus, the failure to detect SMC1α in the RAD21L immunoprecipitates likely reflects the limited amount of RAD21L present in the extract as described above. Moreover, SA2 was coprecipitated with SMC1α, whereas the vast majority STAG3 was coprecipitated with SMC1β. In the final set of experiments, antibodies against the SA–STAG subunits were used for immunoprecipitation (Fig. 7 C). Like kleisin subunits, each of the SA–STAG subunits formed distinctive cohesin complexes. We found that RAD21 associated primarily with SA1 or SA2 ,whereas RAD21L and REC8 associated preferentially with STAG3.

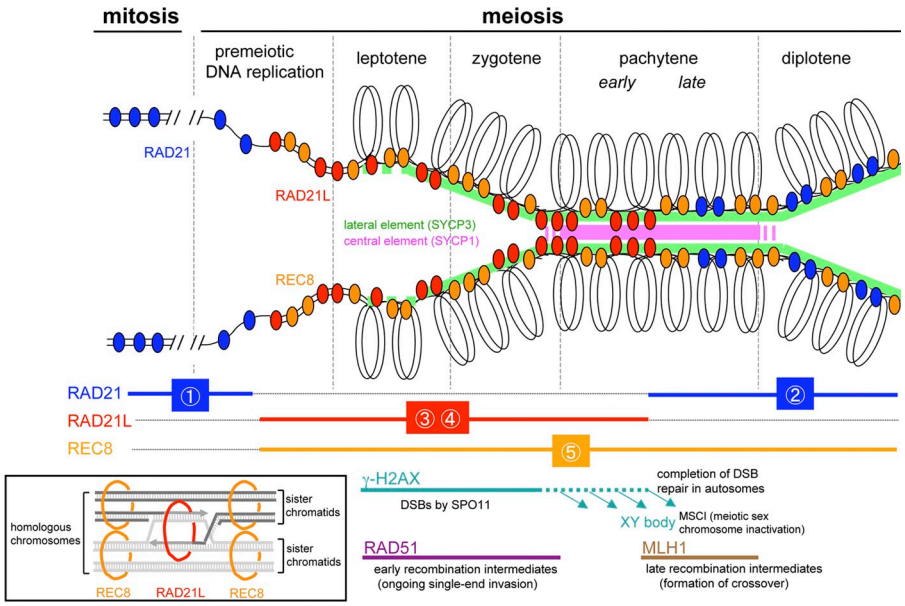

Figure 8. **Spatiotemporal distribution of multiple cohesin complexes in the processes of paring, synapsis, and recombination of homologous chromosomes during meiotic prophase I in mammals.** RAD21-, RAD21L-, and REC8-containing cohesins are indicated by the blue, red, and orange ovals, respectively. Circled numbers correspond to the different cohesin complexes summarized in Fig. 7 E. Although the intriguing possibility is depicted here that cohesin^{RAD21L} could embrace two duplexes from homologous chromosomes whereas cohesin^{REC8} could do so from sister chromatids (inset), our current results by no means exclude other models.

The results described above allow us to conclude that the testis extracts used in the current study contain at least four different meiotic cohesin complexes in addition to the canonical mitotic complexes (Fig. 7 E). In brief, RAD21 and RAD21L can form complexes with both SMC1α and SMC1β, whereas REC8 associates with only SMC1β. Two meiotic kleisin subunits, RAD21L and REC8, associate preferentially with STAG3, whereas RAD21 associates with SA1, SA2, and STAG3. Intriguingly, at least under the current conditions tested, phosphorylation of STAG3 is prominent only when it is complexed with RAD21L.

Discussion

Spatiotemporal distributions of multiple cohesins in mammalian meiosis

In the current study, we report a novel cohesin subunit, referred to as RAD21L, which localizes along the AE/LEs of the SC exclusively from leptotene to mid pachytene in mammalian meiosis. Combined with the expression profiles of known cohesin subunits (Eijpe et al., 2000, 2003; Prieto et al., 2001, 2002, 2004; Revenkova et al., 2001; Lee et al., 2003; Xu et al., 2004), we propose the following diagram in which spatiotemporal coordination of multiple cohesin complexes supports the elaborate sequence of chromosomal events during meiotic prophase I (Fig. 8). According to this scenario, RAD21-containing cohesin (cohesin^{RAD21}) is largely replaced by cohesins containing RAD21L and REC8 (cohesin^{RAD21L} and cohesin^{REC8}, respectively) during premeiotic S phase. Cohesin^{RAD21L} exists as two distinct types: one containing SMC1α and the other SMC1β, whereas cohesin^{REC8} is most likely to represent a single form containing SMC1β (Fig. 7 E). Although cohesin^{RAD21L} apparently colocalizes with cohesin^{REC8} along the AE/LEs by mid pachytene, their detailed distributions do not overlap with each other, implicating the existence of alternating sub-chromosomal domains along the SC. Notably, cohesin^{RAD21L} disappears from the SC after mid pachytene, and is replaced with cohesin^{RAD21}, whereas cohesin^{REC8} stays on meiotic chromosomes. At this and later stages in prophase I, the majority of cohesin^{RAD21} is likely to contain SMC1β rather than SMC1α (Revenkova et al., 2001, 2004).

RAD21L might be involved in synapsis initiation between homologous chromosomes

A previous study using *SYCP3*-deficient (*SYCP3*$^{-/-}$) mice indicated that a cohesin axis is formed even in the absence of the AE (Pelttari et al., 2001). This observation led the authors to propose that the cohesin axis is preformed along each chromosome and acts as the organizing framework for subsequent AE/LE anchorage and formation. On the other hand, in *REC8*$^{-/-}$ or *SMC1β*$^{-/-}$ mice, the AEs are assembled partially (Revenkova et al., 2004; Xu et al., 2005). Because thread-like signals of RAD21L are observed before the appearance of linear signals of SYCP3 (unpublished data), as has been reported for REC8 (Eijpe et al., 2003; Lee et al., 2003), it is reasonable to speculate that RAD21L might act in concert with REC8 to help assemble the AEs on their own axes.

In early zygotene, SYCP1 is recruited to between the two AEs of homologous chromosomes and participates in the assembly of the SC (Meuwissen et al., 1992). What factor(s) might recruit SYCP1 to the AEs and to help initiate synapsis is currently unknown. We suggest that RAD21L would be an excellent candidate for such a factor for the following two reasons. First, RAD21L foci appear enriched at connection sites between two AEs undergoing synapsis at zygotene (Fig. 4, h′ and h′′). Second, our preliminary results show that RAD21L, but neither RAD21 nor REC8, is coimmunoprecipitated with a fraction of SYCP1 (Fig. S4 B). If this hypothesis were correct, then the disappearance of RAD21L at mid pachytene would be an essential prerequisite for starting desynapsis (and to preventing resynapsis) at diplotene.

It is important to note that, unlike RAD21L, all other meiotic cohesin subunits characterized so far (SMC1β, REC8, and STAG3) persist at the inter-sister chromatid regions at least until

the onset of anaphase I when homologous chromosomes start to separate. It is therefore reasonable to assume that they possess the canonical function of cohesins (i.e., holding sister chromatids together) at least in part. Indeed, precocious separation of sister chromatids is observed in *SMC1β*$^{-/-}$ oocytes or oocytes depleted of SGO2, a protector of centromeric REC8 (Revenkova et al., 2004; Hodges et al., 2005; Lee et al., 2008). Interestingly, in *REC8*$^{-/-}$ mice, synapsis occurs between sister chromatids instead of between homologous chromosomes (Xu et al., 2005), implicating that REC8-mediated cohesion between sister chromatids is a prerequisite for proper recognition of homologous chromosomes to initiate their synapsis. The unique behavior of RAD21L reported in the current study indicates that, if RAD21L had a function in holding sister chromatids, it would be limited until mid pachytene. We therefore suggest the alternative (yet not mutually exclusive) possibility that RAD21L uses early recombination intermediates to recognize homologous chromosomes and then holds a pair of nonsister duplexes from homologous chromosomes (Fig. 8, inset). This situation could in turn provide a structural base for recruitment of SYCP1, thereby coupling homologous chromosome pairing to synapsis initiation.

Possible functions of RAD21L in meiotic recombination

The signal of γ-H2AX, a marker for DSBs, initially appears chromatin-widely from leptotene through zygotene, and largely disappears by early pachytene. At this stage, a sub-fraction of the γ-H2AX signal remains on autosomes only at the proximity of RAD21L localizing the SC (Fig. 6 A, c, g, and k). Remarkably, this particular sub-fraction of γ-H2AX and RAD21L disappear highly coincidentally around mid pachytene, and MLH1 foci appear at the same time. Thus, RAD21L apparently persists along the SC until processing of all DSBs is complete. This observation implies that RAD21L may be involved in the processing of recombination intermediates occurring along the SC until mid pachytene. In this context, it is important to ask why RAD21 and RAD21L might appear on chromosomes in a mutually exclusive manner in meiotic prophase I. A recent study shows that RAD21 facilitates recombination between sister chromatids, whereas it suppresses recombination between homologous chromosomes at the same time (Covo et al., 2010). It is tempting to speculate that replacement of RAD21 with RAD21L in early prophase I would help reverse this situation, thereby creating an environment in which recombination between homologous chromosomes becomes preferable. The proposed function of RAD21L to hold two nonsister duplexes from homologous chromosomes (Fig. 8, inset) provides a mechanistic explanation for how RAD21L might promote meiotic recombination. However, we cannot rule out the possibility that RAD21L might be involved in other events occurring during pachytene, such as pachytene checkpoint responses (Roeder and Bailis, 2000), apoptosis of cells defective in meiotic sex chromosome inactivation (Turner, 2007), and deposition of histone H1t (Drabent et al., 1996).

How might RAD21L dissociate from meiotic chromosomes at mid pachytene?

Perhaps one of the most important observations made in the current study is that RAD21L disappears from the SC at mid pachytene. No such behavior has been reported for the canonical cohesin subunits or the canonical SC components (Suja and Barbero, 2009). Moreover, BRCA1 and ATR are localized along unsynapsed AEs (Turner et al., 2004), whereas HORMAD1 and HORMAD2, recently identified HORMA domain–containing proteins, preferentially associate with unsynapsed and desynapsed regions of the AE/LEs (Wojtasz et al., 2009; Fukuda et al., 2010). Thus, the apparent loss of RAD21L at mid pachytene from the fully synapsed chromosomes is exceptionally unique (except the γ-H2AX signal described above).

Then what mechanism might promote the dissociation of RAD21L from the SC at mid pachytene? In mitotic prophase, phosphorylation of the STAG–SA subunits (SA1 and SA2) is known to contribute to the release of cohesins from chromosome arms (Losada et al., 2002; Sumara et al., 2002; Hauf et al., 2005). In the current study, we find that STAG3 associates with the three different kleisin subunits (RAD21, RAD21L, and REC8) in meiosis, but only the fraction of STAG3 associating with RAD21L is phosphorylated. It is therefore possible that phosphorylation of STAG3 contributes to the release of cohesin^{RAD21L} at mid pachytene. However, the current data do not exclude the possibility that STAG3 phosphorylation might regulate other unique functions attributed to cohesin^{RAD21L} on the SC. Another candidate factor that could contribute to the release of cohesin^{RAD21L} is WAPL, a protein that plays a direct role in releasing cohesins from chromosome arms in mitotic prophase (Gandhi et al., 2006; Kueng et al., 2006; Shintomi and Hirano, 2009). Interestingly, mouse WAPL has been localized along the SC in pachytene spermatocytes (Kuroda et al., 2005), making the possibility highly plausible that WAPL also functions as a key regulator of meiotic cohesins, including cohesin^{RAD21L}. Future studies should explore this possibility.

Are RAD21L equivalents present in invertebrate species?

In *Drosophila*, male meiosis involves neither SC formation nor meiotic recombination. Although the SC is formed in female meiosis, homologous synapsis does not depend on DSBs or recombination (Page and Hawley, 2004). Curiously, no putative orthologue of REC8 has been identified in *Drosophila*. Instead, C(2)M, a protein that has been reported to have a very limited similarity to kleisins, is expressed specifically in meiosis (Manheim and McKim, 2003; Schleiffer et al., 2003), and may function together with SMC3 (Heidmann et al., 2004). C(2)M is localized in the central region adjacent to the LEs, and is required for both the assembly of the CE component C(3)G and proper formation of crossovers (Manheim and McKim, 2003; Anderson et al., 2005). It is very interesting to note that C(2)M disappears from the SC in late pachytene (Manheim and McKim, 2003; Heidmann et al., 2004). This particular feature and the proposed function of C(2)M are highly reminiscent of those of mouse RAD21L reported in the current study. We therefore suggest that the "functional homologue" of *Drosophila* C(2)M in vertebrates could indeed be RAD21L rather than REC8. REC8-equivalent functions could be assigned to other chromosomal proteins in *Drosophila,* such as ORD and SOLO, although neither of them displays any similarity to cohesin

subunits at the primary structure level (Webber et al., 2004; Yan et al., 2010).

Like female *Drosophila*, *Caenorhabditis elegans* does not require DSBs for alignment or synapsis of homologous chromosomes (Bhalla and Dernburg, 2008). In *C. elegans*, three kleisin subunits (REC-8, COH-3, and COH-4) apparently cooperate to support cohesion-related functions by meiosis I, although REC-8 alone is sufficient for sister centromere cohesion in meiosis II (Severson et al., 2009). Therefore, either one or both COH-3 and COH-4 could play a role similar to that of *Drosophila* C(2)M and vertebrate RAD21L. Given their highly divergent primary sequences, however, neither C(2)M nor COH-3 or COH-4 is to be placed at the position of the "RAD21L orthologues." It is most likely that they might have acquired related if not identical functions through convergent evolution. Whatever the precise relationship might be, our finding of RAD21L in vertebrates shed new light on the mechanism by which intricate combinations of cohesins and noncohesin components have evolved to support the fundamental program that ultimately creates physical connections between homologous chromosomes in meiosis.

Conclusion

The present study illuminates the molecular mechanism by which concerted actions of multiple forms of cohesins contribute to the progression of a series of meiotic events, e.g., pairing, synapsis, and recombination of homologous chromosomes and repair of DSBs. In vertebrates, RAD21L might have evolved as a conductor that orchestrates a series of complicated events to proceed in a timely and organized fashion. To test the proposed functions of RAD21L, we are now embarking on the generation of *RAD21L* knockout mice.

Materials and methods

Animal study compliance

All animal experiment protocols used in the present study have been approved by the Director of RIKEN Wako Institute, following a review by the Wako Animal Experiment Committee.

Cloning of mRAD21L cDNA

Single-stranded cDNAs were generated from total RNA extracted from testes of an adult C57BL/6 mouse with Superscript III reverse transcription (Invitrogen). The resultant cDNAs were used as a template for PCR to amplify the cDNA sequence encoding a hypothetical protein (NCBI Protein database accession no. NM_001114677), referred to here as RAD21L. The following primers were designed and used for RT-PCR: 5′-ATGTTCTACACTCATGTGCT-3′ and 5′-TCACATCTTATAGAACATTG-3′. The PCR products were cloned into pGEM-T-Easy vector (Promega) and then subjected to sequence analysis. The nucleotide sequence data will appear in the GenBank/EMBL/DDBJ databases with the accession no. AB574185.

Quantitative real-time RT-PCR

Total RNAs from liver, spleen, and testes of 7–10-wk-old C57BL/6 mice (Agilent Technologies) were treated with TURBO DNase (Applied Biosystems) to remove contaminating genomic DNAs. Using the RNAs as a template, single-stranded cDNAs were generated and used for real-time PCR. Quantitative analysis of gene expression was performed using a Fast Real-Time PCR System (model 7900HT; Applied Biosystems) in 30 µl of total reaction volume containing 100 ng of cDNAs with 250 nM TaqMan probes and 900 nM forward and reverse primers. The probes and primers used for the analysis are listed in Table S1. As an internal control, gene expression of *GAPDH* was also monitored using its probe and primers (4352339E; Life Technologies). Standard curves for each gene were drawn by plotting the Ct (threshold cycles) values (Y axis) against the log of cDNA amount (X axis) through conduction of real-time PCR using a serial dilution of a known amount of testis cDNA. The standard curves and accompanying amplification efficiencies in PCR for each gene are used for rough estimation of the relative amount of each gene transcript in a testis.

Antibodies

To produce specific antisera, C-terminal fragments of mouse RAD21 (290–635 aa), mouse RAD21L (185–552 aa), and mouse REC8 (250–591 aa) were expressed in *E. coli*, purified, and used as antigens to immunize rabbits or rats. The anti-RAD21L and anti-REC8 antisera were passed through a column conjugated with the recombinant fragment of RAD21 to remove fractions potentially cross-reacting with RAD21. Likewise, the anti-RAD21 antiserum was passed through a column conjugated with recombinant RAD21L. Then, the flow-through fractions were loaded onto columns conjugated with their own antigens, and specific antibodies bound to the columns were purified. Rabbits were also immunized with a synthetic peptide containing the C-terminal 18 amino acids of mouse SMC1β to produce polyclonal antisera. Other antibodies used in this study were described elsewhere or purchased from companies: anti-hSMC1 antibody (Gandhi et al., 2006); anti-XSMC3, anti-XSA1, anti-XSA2 antibodies (Losada et al., 1998); anti-SYCP3 antibody (Lee et al., 2003); anti-SYCP1 antibody (ab15087) and anti-MSH4 antibody (ab58666) from Abcam; anti-H2AX phosphorylated (Ser139) antibody (613401) from BioLegend; and anti-RAD51 antibody (sc-8349), anti-STAG3 antibody (sc-20341), anti-PCNA antibody (sc-56), and anti-MLH1 antibody (sc-133203) from Santa Cruz Biotechnology, Inc.

Preparation of extracts from organs

Various organs were collected from 3-mo-old mice and minced with a surgical blade. 50 mg of each sample was homogenized with a pestle, sonicated, and boiled for 3 min in 500 µl of 1x SDS sample buffer (62.5 mM Tris-HCl, pH 6.8, 1% SDS, 10% glycerol, 50 mM DTT, and 0.02% bromophenol blue). After centrifugation at 9,100 *g* for 10 min at 4°C, the supernatant was collected and used for immunoblot analysis.

For immunoprecipitation analysis, whole extracts from testes of 8–10-wk-old mice were prepared as follows. Five pairs of testis were removed, decapsulated surgically, and homogenized with a Dounce homogenizer in 10 ml of extraction buffer (20 mM Tris-HCl, pH 7.4, 150 mM NaCl, 2 mM EDTA, 1% Nonidet P-40, 1% Na deoxycholate, 0.1% SDS, 50 mM NaF, 1 mM Na_3VO_4, and 5 mM 2-mercaptoethanol) supplemented with a Protease Inhibitor Cocktail tablet (Roche). The homogenized solution was sonicated and centrifuged at 200,000 *g* for 30 min at 4°C, and the supernatant was collected and used as testis extracts.

Immunoprecipitation and immunoblotting

For immunoprecipitations, testis extracts were incubated with one of the antibodies against cohesin subunits for 1.5 h at 4°C with rotor agitation. After the addition of rProtein A Sepharose (GE Healthcare), the extracts were further incubated for 1 h; the beads were then washed five times with the extraction buffer, and the immunoprecipitates were analyzed by SDS-PAGE followed by immunoblotting. The signals were detected using either Immobilon Western Chemilluminescent HRP Substrate (Millipore) or Super-Signal West Femto Maximum Sensitivity Substrate (Thermo Fisher Scientific). For protein phosphatase treatment (Fig. 7 D), immunoprecipitates obtained with anti-RAD21L antibody were washed five times with the extraction buffer and twice with 1x λ-protein phosphatase (λ-PPase) buffer, then incubated with 20 U/µl λ-PPase (New England Biolabs, Inc.) in the buffer for 30 min at 30°C. As a control, the immunoprecipitates were incubated without λ-PPase in the buffer. Then the immunoprecipitates were subjected to immunoblot analysis with anti-STAG3 and anti-RAD21L antibodies.

Immunofluorescent labeling

Testes or ovaries were frozen in O.C.T. Compound Embedding medium (Sakura) and kept at −80°C until use. Cryostat sections of 10-µm thickness were prepared at −20°C, air dried on MAS-GP–coated slides (Matsunami), and fixed in 1% paraformaldehyde in PBS for 10 min. After washing with PBS three times, the sections were incubated with primary antibodies at appropriate dilutions in 1% BSA in PBS at 4°C overnight. After washing three times with PBS, the sections were incubated with secondary antibodies (Alexa 488– or 568–conjugated anti–mouse, anti–rat, or anti–rabbit IgG antibodies; Invitrogen) at 1:500 dilution at room temperature for 1 h. DNA was counterstained with Hoechst 34580 (Invitrogen).

Meiotic nuclear spreads were prepared according to the methods described previously (Lee et al., 2003). In brief, testicular cells were put on poly-L-lysine–coated coverslips. The cells on the coverslips were placed in

85 mM NaCl for 3 min, and fixed in 1% paraformaldehyde solution (pH 8.2 adjusted with 10 mM sodium borate) for 15 min. The coverslips were rinsed three times for 1 min each with 4% (vol/vol) Photo-Flo (Kodak) in distilled water (pH 8.0) and air dried overnight. The nuclear spreads on coverslips were placed in PBS for 10 min, in 1 µg/ml DNase I (Sigma-Aldrich) in PBS for 20 min, in a detergent solution (5 mM EDTA, 0.25% gelatin, and 0.05% Triton X-100 in PBS) for 10 min, in PBS for 10 min, and finally in a blocking buffer (3% BSA and 0.05% Triton X-100 in PBS) for 30 min. The samples were incubated with the primary antibodies at appropriate dilutions in the blocking buffer at 4°C overnight, and washed with PBS for 10 min, with the detergent solution for 10 min, and with PBS for 10 min. The coverslips were then incubated with the secondary antibodies at appropriate dilutions in the blocking buffer. DNA was counterstained with Hoechst 34580. The samples were mounted with VECTASHIELD Mounting Medium (Vector Laboratories) and observed under a confocal microscope (model LSM710; Carl Zeiss, Inc.) with a Plan Apochromat 20x/0.8 or 100x/1.46 oil DIC objective lens. All images were obtained by scanning a single section of samples using ZEN2008 software (Carl Zeiss, Inc.) and imported into Photoshop (Adobe). Then gamma adjustment was performed for each of the RGB channels. For double labeling of RAD21L and REC8 (Fig. 5), chromosome spreads were treated simultaneously with a mixture of the two primary antibodies. We also tested sequential treatments with the two antibodies and obtained exactly the same result, eliminating the possibility that they may compete with each other for a common epitope.

Online supplemental material

Fig. S1 shows the alignment of amino acid sequences between mouse RAD21, RAD21L, and REC8. Fig. S2 shows that RAD21L appears in premeiotic S phase. Fig. S3 shows the relative timing of the disappearance of RAD21L and RAD51 or MSH4 from the synaptonemal complex. Fig. S4 shows that the relative amount of RAD21L is extremely low compared with other kleisin subunits in testis and that RAD21L is coimmunoprecipitated with a fraction of SYCP1. Table S1 shows probes and primers used for quantitative real-time PCR. Online supplemental material is available at http://www.jcb.org/cgi/content/full/jcb.201008005/DC1.

We thank A. Matsuura for her contribution to production of antibodies. We are also grateful to the Support Units for Bio-material Analysis and for Animal Experiment, RIKEN BSI Resources Center, for help with sequence and real-time RT-PCR analyses and for production of rat polyclonal antibodies. We thank all the members of our laboratory for critically reading the manuscript.

This work was supported by Grant-in-Aids for Young Scientists (B) (20780203) to J.Lee and for Specially Promoted Research (20002010) to T. Hirano.

Submitted: 2 August 2010
Accepted: 22 December 2010

References

Anderson, L.K., A. Reeves, L.M. Webb, and T. Ashley. 1999. Distribution of crossing over on mouse synaptonemal complexes using immunofluorescent localization of MLH1 protein. *Genetics.* 151:1569–1579.

Anderson, L.K., S.M. Royer, S.L. Page, K.S. McKim, A. Lai, M.A. Lilly, and R.S. Hawley. 2005. Juxtaposition of C(2)M and the transverse filament protein C(3)G within the central region of *Drosophila* synaptonemal complex. *Proc. Natl. Acad. Sci. USA.* 102:4482–4487. doi:10.1073/pnas.0500172102

Barchi, M., S. Mahadevaiah, M. Di Giacomo, F. Baudat, D.G. de Rooij, P.S. Burgoyne, M. Jasin, and S. Keeney. 2005. Surveillance of different recombination defects in mouse spermatocytes yields distinct responses despite elimination at an identical developmental stage. *Mol. Cell. Biol.* 25:7203–7215. doi:10.1128/MCB.25.16.7203-7215.2005

Bellani, M.A., P.J. Romanienko, D.A. Cairatti, and R.D. Camerini-Otero. 2005. SPO11 is required for sex-body formation, and Spo11 heterozygosity rescues the prophase arrest of Atm−/− spermatocytes. *J. Cell Sci.* 118:3233–3245. doi:10.1242/jcs.02466

Bhalla, N., and A.F. Dernburg. 2008. Prelude to a division. *Annu. Rev. Cell Dev. Biol.* 24:397–424. doi:10.1146/annurev.cellbio.23.090506.123245

Blanco-Rodríguez, J. 2009. gammaH2AX marks the main events of the spermatogenic process. *Microsc. Res. Tech.* 72:823–832. doi:10.1002/jemt.20730

Bravo, R., and H. Macdonald-Bravo. 1987. Existence of two populations of cyclin/proliferating cell nuclear antigen during the cell cycle: association with DNA replication sites. *J. Cell Biol.* 105:1549–1554. doi:10.1083/jcb.105.4.1549

Chicheportiche, A., J. Bernardino-Sgherri, B. de Massy, and B. Dutrillaux. 2007. Characterization of Spo11-dependent and independent phospho-H2AX foci during meiotic prophase I in the male mouse. *J. Cell Sci.* 120:1733–1742. doi:10.1242/jcs.004945

Covo, S., J.W. Westmoreland, D.A. Gordenin, and M.A. Resnick. 2010. Cohesin Is limiting for the suppression of DNA damage-induced recombination between homologous chromosomes. *PLoS Genet.* 6:e1001006. doi:10.1371/journal.pgen.1001006

de Boer, E., and C. Heyting. 2006. The diverse roles of transverse filaments of synaptonemal complexes in meiosis. *Chromosoma.* 115:220–234. doi:10.1007/s00412-006-0057-5

de Vries, F.A., E. de Boer, M. van den Bosch, W.M. Baarends, M. Ooms, L. Yuan, J.G. Liu, A.A. van Zeeland, C. Heyting, and A. Pastink. 2005. Mouse Sycp1 functions in synaptonemal complex assembly, meiotic recombination, and XY body formation. *Genes Dev.* 19:1376–1389. doi:10.1101/gad.329705

Dobson, M.J., R.E. Pearlman, A. Karaiskakis, B. Spyropoulos, and P.B. Moens. 1994. Synaptonemal complex proteins: occurrence, epitope mapping and chromosome disjunction. *J. Cell Sci.* 107:2749–2760.

Drabent, B., C. Bode, B. Bramlage, and D. Doenecke. 1996. Expression of the mouse testicular histone gene H1t during spermatogenesis. *Histochem. Cell Biol.* 106:247–251. doi:10.1007/BF02484408

Eijpe, M., C. Heyting, B. Gross, and R. Jessberger. 2000. Association of mammalian SMC1 and SMC3 proteins with meiotic chromosomes and synaptonemal complexes. *J. Cell Sci.* 113:673–682.

Eijpe, M., H. Offenberg, R. Jessberger, E. Revenkova, and C. Heyting. 2003. Meiotic cohesin REC8 marks the axial elements of rat synaptonemal complexes before cohesins SMC1beta and SMC3. *J. Cell Biol.* 160:657–670. doi:10.1083/jcb.200212080

Fukuda, T., K. Daniel, L. Wojtasz, A. Toth, and C. Höög. 2010. A novel mammalian HORMA domain-containing protein, HORMAD1, preferentially associates with unsynapsed meiotic chromosomes. *Exp. Cell Res.* 316:158–171. doi:10.1016/j.yexcr.2009.08.007

Gandhi, R., P.J. Gillespie, and T. Hirano. 2006. Human Wapl is a cohesin-binding protein that promotes sister-chromatid resolution in mitotic prophase. *Curr. Biol.* 16:2406–2417. doi:10.1016/j.cub.2006.10.061

Guillon, H., F. Baudat, C. Grey, R.M. Liskay, and B. de Massy. 2005. Crossover and noncrossover pathways in mouse meiosis. *Mol. Cell.* 20:563–573. doi:10.1016/j.molcel.2005.09.021

Hauf, S., E. Roitinger, B. Koch, C.M. Dittrich, K. Mechtler, and J.M. Peters. 2005. Dissociation of cohesin from chromosome arms and loss of arm cohesion during early mitosis depends on phosphorylation of SA2. *PLoS Biol.* 3:e69. doi:10.1371/journal.pbio.0030069

Heidmann, D., S. Horn, S. Heidmann, A. Schleiffer, K. Nasmyth, and C.F. Lehner. 2004. The *Drosophila* meiotic kleisin C(2)M functions before the meiotic divisions. *Chromosoma.* 113:177–187. doi:10.1007/s00412-004-0305-5

Hirano, T. 2006. At the heart of the chromosome: SMC proteins in action. *Nat. Rev. Mol. Cell Biol.* 7:311–322. doi:10.1038/nrm1909

Hodges, C.A., E. Revenkova, R. Jessberger, T.J. Hassold, and P.A. Hunt. 2005. SMC1beta-deficient female mice provide evidence that cohesins are a missing link in age-related nondisjunction. *Nat. Genet.* 37:1351–1355. doi:10.1038/ng1672

Hunter, N., and N. Kleckner. 2001. The single-end invasion: an asymmetric intermediate at the double-strand break to double-holliday junction transition of meiotic recombination. *Cell.* 106:59–70. doi:10.1016/S0092-8674(01)00430-5

Keeney, S. 2001. Mechanism and control of meiotic recombination initiation. *Curr. Top. Dev. Biol.* 52:1–53. doi:10.1016/S0070-2153(01)52008-6

Kueng, S., B. Hegemann, B.H. Peters, J.J. Lipp, A. Schleiffer, K. Mechtler, and J.M. Peters. 2006. Wapl controls the dynamic association of cohesin with chromatin. *Cell.* 127:955–967. doi:10.1016/j.cell.2006.09.040

Kuroda, M., K. Oikawa, T. Ohbayashi, K. Yoshida, K. Yamada, J. Mimura, Y. Matsuda, Y. Fujii-Kuriyama, and K. Mukai. 2005. A dioxin sensitive gene, mammalian WAPL, is implicated in spermatogenesis. *FEBS Lett.* 579:167–172. doi:10.1016/j.febslet.2004.11.070

Lee, J., T. Yokota, and M. Yamashita. 2002. Analyses of mRNA expression patterns of cohesin subunits Rad21 and Rec8 in mice: germ cell-specific expression of rec8 mRNA in both male and female mice. *Zoolog. Sci.* 19:539–544. doi:10.2108/zsj.19.539

Lee, J., T. Iwai, T. Yokota, and M. Yamashita. 2003. Temporally and spatially selective loss of Rec8 protein from meiotic chromosomes during mammalian meiosis. *J. Cell Sci.* 116:2781–2790. doi:10.1242/jcs.00495

Lee, J., T.S. Kitajima, Y. Tanno, K. Yoshida, T. Morita, T. Miyano, M. Miyake, and Y. Watanabe. 2008. Unified mode of centromeric protection by shugoshin in mammalian oocytes and somatic cells. *Nat. Cell Biol.* 10:42–52. doi:10.1038/ncb1667

Losada, A., M. Hirano, and T. Hirano. 1998. Identification of *Xenopus* SMC protein complexes required for sister chromatid cohesion. *Genes Dev.* 12:1986–1997. doi:10.1101/gad.12.13.1986

Losada, A., T. Yokochi, R. Kobayashi, and T. Hirano. 2000. Identification and characterization of SA/Scc3p subunits in the *Xenopus* and human cohesin complexes. *J. Cell Biol.* 150:405–416. doi:10.1083/jcb.150.3.405

Losada, A., M. Hirano, and T. Hirano. 2002. Cohesin release is required for sister chromatid resolution, but not for condensin-mediated compaction, at the onset of mitosis. *Genes Dev.* 16:3004–3016. doi:10.1101/gad.249202

Mahadevaiah, S.K., J.M. Turner, F. Baudat, E.P. Rogakou, P. de Boer, J. Blanco-Rodríguez, M. Jasin, S. Keeney, W.M. Bonner, and P.S. Burgoyne. 2001. Recombinational DNA double-strand breaks in mice precede synapsis. *Nat. Genet.* 27:271–276. doi:10.1038/85830

Manheim, E.A., and K.S. McKim. 2003. The Synaptonemal complex component C(2)M regulates meiotic crossing over in *Drosophila*. *Curr. Biol.* 13:276–285. doi:10.1016/S0960-9822(03)00050-2

Meuwissen, R.L., H.H. Offenberg, A.J. Dietrich, A. Riesewijk, M. van Iersel, and C. Heyting. 1992. A coiled-coil related protein specific for synapsed regions of meiotic prophase chromosomes. *EMBO J.* 11:5091–5100.

Miyazaki, W.Y., and T.L. Orr-Weaver. 1994. Sister-chromatid cohesion in mitosis and meiosis. *Annu. Rev. Genet.* 28:167–187.

Nasmyth, K., and C.H. Haering. 2009. Cohesin: its roles and mechanisms. *Annu. Rev. Genet.* 43:525–558. doi:10.1146/annurev-genet-102108-134233

Offenberg, H.H., J.A. Schalk, R.L. Meuwissen, M. van Aalderen, H.A. Kester, A.J. Dietrich, and C. Heyting. 1998. SCP2: a major protein component of the axial elements of synaptonemal complexes of the rat. *Nucleic Acids Res.* 26:2572–2579. doi:10.1093/nar/26.11.2572

Page, S.L., and R.S. Hawley. 2004. The genetics and molecular biology of the synaptonemal complex. *Annu. Rev. Cell Dev. Biol.* 20:525–558. doi:10.1146/annurev.cellbio.19.111301.155141

Pelttari, J., M.R. Hoja, L. Yuan, J.G. Liu, E. Brundell, P. Moens, S. Santucci-Darmanin, R. Jessberger, J.L. Barbero, C. Heyting, and C. Höög. 2001. A meiotic chromosomal core consisting of cohesin complex proteins recruits DNA recombination proteins and promotes synapsis in the absence of an axial element in mammalian meiotic cells. *Mol. Cell. Biol.* 21:5667–5677. doi:10.1128/MCB.21.16.5667-5677.2001

Petronczki, M., M.F. Siomos, and K. Nasmyth. 2003. Un ménage à quatre: the molecular biology of chromosome segregation in meiosis. *Cell.* 112:423–440. doi:10.1016/S0092-8674(03)00083-7

Plug, A.W., A.H. Peters, K.S. Keegan, M.F. Hoekstra, P. de Boer, and T. Ashley. 1998. Changes in protein composition of meiotic nodules during mammalian meiosis. *J. Cell Sci.* 111:413–423.

Prieto, I., J.A. Suja, N. Pezzi, L. Kremer, C. Martínez-A, J.S. Rufas, and J.L. Barbero. 2001. Mammalian STAG3 is a cohesin specific to sister chromatid arms in meiosis I. *Nat. Cell Biol.* 3:761–766. doi:10.1038/35087082

Prieto, I., N. Pezzi, J.M. Buesa, L. Kremer, I. Barthelemy, C. Carreiro, F. Roncal, A. Martinez, L. Gomez, R. Fernandez, et al. 2002. STAG2 and Rad21 mammalian mitotic cohesins are implicated in meiosis. *EMBO Rep.* 3:543–550. doi:10.1093/embo-reports/kvf108

Prieto, I., C. Tease, N. Pezzi, J.M. Buesa, S. Ortega, L. Kremer, A. Martínez, C. Martínez-A, M.A. Hultén, and J.L. Barbero. 2004. Cohesin component dynamics during meiotic prophase I in mammalian oocytes. *Chromosome Res.* 12:197–213. doi:10.1023/B:CHRO.0000021945.83198.0e

Putnam, N.H., T. Butts, D.E. Ferrier, R.F. Furlong, U. Hellsten, T. Kawashima, M. Robinson-Rechavi, E. Shoguchi, A. Terry, J.K. Yu, et al. 2008. The amphioxus genome and the evolution of the chordate karyotype. *Nature*. 453:1064–1071. doi:10.1038/nature06967

Revenkova, E., M. Eijpe, C. Heyting, B. Gross, and R. Jessberger. 2001. Novel meiosis-specific isoform of mammalian SMC1. *Mol. Cell. Biol.* 21:6984–6998. doi:10.1128/MCB.21.20.6984-6998.2001

Revenkova, E., M. Eijpe, C. Heyting, C.A. Hodges, P.A. Hunt, B. Liebe, H. Scherthan, and R. Jessberger. 2004. Cohesin SMC1 beta is required for meiotic chromosome dynamics, sister chromatid cohesion and DNA recombination. *Nat. Cell Biol.* 6:555–562. doi:10.1038/ncb1135

Roeder, G.S., and J.M. Bailis. 2000. The pachytene checkpoint. *Trends Genet.* 16:395–403. doi:10.1016/S0168-9525(00)02080-1

Santucci-Darmanin, S., D. Walpita, F. Lespinasse, C. Desnuelle, T. Ashley, and V. Paquis-Flucklinger. 2000. MSH4 acts in conjunction with MLH1 during mammalian meiosis. *FASEB J.* 14:1539–1547. doi:10.1096/fj.14.11.1539

Schleiffer, A., S. Kaitna, S. Maurer-Stroh, M. Glotzer, K. Nasmyth, and F. Eisenhaber. 2003. Kleisins: a superfamily of bacterial and eukaryotic SMC protein partners. *Mol. Cell.* 11:571–575. doi:10.1016/S1097-2765(03)00108-4

Schwacha, A., and N. Kleckner. 1997. Interhomolog bias during meiotic recombination: meiotic functions promote a highly differentiated interhomolog-only pathway. *Cell.* 90:1123–1135. doi:10.1016/S0092-8674(00)80378-5

Severson, A.F., L. Ling, V. van Zuylen, and B.J. Meyer. 2009. The axial element protein HTP-3 promotes cohesin loading and meiotic axis assembly in C. elegans to implement the meiotic program of chromosome segregation. *Genes Dev.* 23:1763–1778. doi:10.1101/gad.1808809

Shintomi, K., and T. Hirano. 2009. Releasing cohesin from chromosome arms in early mitosis: opposing actions of Wapl-Pds5 and Sgo1. *Genes Dev.* 23:2224–2236. doi:10.1101/gad.1844309

Suja, J.A., and J.L. Barbero. 2009. Cohesin complexes and sister chromatid cohesion in mammalian meiosis. *Genome Dyn.* 5:94–116. doi:10.1159/000166622

Sumara, I., E. Vorlaufer, P.T. Stukenberg, O. Kelm, N. Redemann, E.A. Nigg, and J.M. Peters. 2002. The dissociation of cohesin from chromosomes in prophase is regulated by Polo-like kinase. *Mol. Cell.* 9:515–525. doi:10.1016/S1097-2765(02)00473-2

Tarsounas, M., T. Morita, R.E. Pearlman, and P.B. Moens. 1999. RAD51 and DMC1 form mixed complexes associated with mouse meiotic chromosome cores and synaptonemal complexes. *J. Cell Biol.* 147:207–220. doi:10.1083/jcb.147.2.207

Turner, J.M.A. 2007. Meiotic sex chromosome inactivation. *Development.* 134:1823–1831. doi:10.1242/dev.000018

Turner, J.M., O. Aprelikova, X. Xu, R. Wang, S. Kim, G.V. Chandramouli, J.C. Barrett, P.S. Burgoyne, and C.X. Deng. 2004. BRCA1, histone H2AX phosphorylation, and male meiotic sex chromosome inactivation. *Curr. Biol.* 14:2135–2142. doi:10.1016/j.cub.2004.11.032

Webber, H.A., L. Howard, and S.E. Bickel. 2004. The cohesion protein ORD is required for homologue bias during meiotic recombination. *J. Cell Biol.* 164:819–829. doi:10.1083/jcb.200310077

Wojtasz, L., K. Daniel, I. Roig, E. Bolcun-Filas, H. Xu, V. Boonsanay, C.R. Eckmann, H.J. Cooke, M. Jasin, S. Keeney, et al. 2009. Mouse HORMAD1 and HORMAD2, two conserved meiotic chromosomal proteins, are depleted from synapsed chromosome axes with the help of TRIP13 AAA-ATPase. *PLoS Genet.* 5:e1000702. doi:10.1371/journal.pgen.1000702

Xu, H., M. Beasley, S. Verschoor, A. Inselman, M.A. Handel, and M.J. McKay. 2004. A new role for the mitotic RAD21/SCC1 cohesin in meiotic chromosome cohesion and segregation in the mouse. *EMBO Rep.* 5:378–384. doi:10.1038/sj.embor.7400121

Xu, H., M.D. Beasley, W.D. Warren, G.T. van der Horst, and M.J. McKay. 2005. Absence of mouse REC8 cohesin promotes synapsis of sister chromatids in meiosis. *Dev. Cell.* 8:949–961. doi:10.1016/j.devcel.2005.03.018

Yan, R., S.E. Thomas, J.H. Tsai, Y. Yamada, and B.D. McKee. 2010. SOLO: a meiotic protein required for centromere cohesion, coorientation, and SMC1 localization in *Drosophila melanogaster*. *J. Cell Biol.* 188:335–349. doi:10.1083/jcb.200904040

Yang, F., R. De La Fuente, N.A. Leu, C. Baumann, K.J. McLaughlin, and P.J. Wang. 2006. Mouse SYCP2 is required for synaptonemal complex assembly and chromosomal synapsis during male meiosis. *J. Cell Biol.* 173:497–507. doi:10.1083/jcb.200603063

Yuan, L., J.G. Liu, J. Zhao, E. Brundell, B. Daneholt, and C. Höög. 2000. The murine SCP3 gene is required for synaptonemal complex assembly, chromosome synapsis, and male fertility. *Mol. Cell.* 5:73–83. doi:10.1016/S1097-2765(00)80404-9